



# Convergent Adaptation of Ootheca Formation as a Reproductive Strategy in Polyneoptera

Erxia Du,<sup>†,1,2,3</sup> Shuai Wang,<sup>†,1</sup> Yun-Xia Luan <sup>†,1</sup> Caisheng Zhou,<sup>†,1</sup> Zhaoxin Li,<sup>†,1</sup> Na Li,<sup>\*,1,3</sup> Shutang Zhou,<sup>\*,4</sup> Tingting Zhang,<sup>5,6</sup> Wentao Ma,<sup>1</sup> Yingying Cui,<sup>1</sup> Dongwei Yuan,<sup>1</sup> Chonghua Ren,<sup>1</sup> Jianzhen Zhang,<sup>5</sup> Siegfried Roth,<sup>6</sup> and Sheng Li <sup>\*,1,2,3</sup>

<sup>1</sup>Guangdong Provincial Key Laboratory of Insect Developmental Biology and Applied Technology, Institute of Insect Science and Technology & School of Life Sciences, South China Normal University, Guangzhou, China

<sup>2</sup>Guangdong Laboratory for Lingnan Modern Agriculture, Guangzhou, China

<sup>3</sup>Guangdong Provincial Key Laboratory of Insect Developmental Biology and Applied Technology, Guangmeiyuan R&D Center, South China Normal University, Meizhou, China

<sup>4</sup>Key Laboratory of Plant Stress Biology, State Key Laboratory of Cotton Biology, School of Life Sciences, Henan University, Kaifeng, China

<sup>5</sup>Research Institute of Applied Biology, Shanxi University, Taiyuan, China

<sup>6</sup>Institute for Zoology, University of Cologne, Cologne, Germany

<sup>†</sup>These authors contributed equally to this work.

\***Corresponding authors:** E-mails: lisheng@scnu.edu.cn; lina5hs@m.scnu.edu.cn; szhou@henu.edu.cn.

**Associate editor:** Patricia Wittkopp

## Abstract

Insects have evolved numerous adaptations and colonized diverse terrestrial environments. Several polyneopterans, including dictyopterans (cockroaches and mantids) and locusts, have developed oothecae, but little is known about the molecular mechanism, physiological function, and evolutionary significance of ootheca formation. Here, we demonstrate that the cockroach asymmetric colleterial glands produce vitellogenins, proline-rich protein, and glycine-rich protein as major ootheca structural proteins (OSPs) that undergo sclerotization and melanization for ootheca formation through the cooperative protocatechuic acid pathway and dopachrome and dopaminechrome subpathway. Functionally, OSP sclerotization and melanization prevent eggs from losing water at warm and dry conditions, and thus effectively maintain embryo viability. Dictyopterans and locusts convergently evolved vitellogenins, apolipoprotein D, and laminins as OSFs, whereas within Dictyoptera, cockroaches and mantids independently developed glycine-rich protein and fibroins as OSFs. Highlighting the ecological-evolutionary importance, convergent ootheca formation represents a successful reproductive strategy in Polyneoptera that promoted the radiation and establishment of cockroaches, mantids, and locusts.

**Key words:** biodiversity, developmental biology, reproduction biology, adaptive biology, insect evolution, evo–devo.

## Introduction

Insects are the most diverse group of animals on the planet, living in nearly all environments. Since their origin approximately 480 Ma, insects have evolved multiple survival strategies (e.g., wings and metamorphosis) with the environmental changes (Misof et al. 2014; Nicholson et al. 2014). The success of insect biodiversity is partially due to their high fecundity, which helped them colonize diverse and harsh terrestrial conditions. Insects lay eggs either individually or in groups, and various egg-laying strategies are essential to survival and fitness in different orders and suborders of insects (Church et al. 2019). A specific example of egg grouping is the ootheca, which is usually referred to as the egg capsule, egg pod, egg sac, or egg case. The hardened and tanned ootheca covers numerous eggs in a highly ordered arrangement and likely protects the eggs from predators, parasitoids,

pathogens, water loss, and other environmental sources of injury (Bell and Adiyodi 1981; Hopkins et al. 1999; Courent et al. 2008). Ootheca mainly occurs in Polyneoptera, most notably in Dictyoptera, including mantids (Mantodea) (Walker et al. 2012) and cockroaches (Blattodea), but has lost in most termites except the basal termite *Mastotermes darwiniensis* (Courent et al. 2008). In Orthoptera, crickets (Orthoptera: Ensifera) do not produce any ootheca, but locusts (Orthoptera: Caelifera) produce, and their ootheca morphology is quite different from dictyopterans. In other groups of Polyneoptera, ootheca has been found in gladiators (Mantophasmatodea, the smallest insect order living in Africa) (Machida et al. 2004; Tojo et al. 2004; Gillott 2005; Roth et al. 2014; Küpper et al. 2019) and a single species of stick insects (Phasmatodea, Goldberg et al. 2015). Such a discontinuous distribution pattern indicates that ootheca is a convergence in egg-laying strategy across polyneopterans

(Church et al. 2019) (supplementary fig. S1, Supplementary Material online). In addition, ootheca sporadically distributes in individual species of Ephemeroptera, Odonata, Hemiptera, Coleoptera, and Diptera (Needham and Heywood 1929; Needham and Westfall 1955; Huang et al. 2006; Flowers and Chaboo 2015; Malek et al. 2019), which strongly suggests that insect ootheca evolved multiple times independently as referred from the parsimony principle in ecology and evolution (Crisci 1982; Coelho et al. 2019).

During the early and middle 20th century, ootheca formation was extensively studied in the American cockroach *Periplaneta americana* (Bell and Adiyodi 1981), an invasive urban pest in the tropics and subtropics. The cockroach ootheca is an oblong and semicylindrical structure that undergoes a rapid and irreversible process of hardening and tanning upon oviposition. The asymmetric colleterial glands (CGs; or female accessory glands; large left CG, LCG; small right CG, RCG) open into the genital vestibulum, and their secretions mix, leading to the formation of ootheca that normally assembles 16 eggs. Each CG contains both secretory and epithelial cells of different subtypes (Bell and Adiyodi 1981; Courrent et al. 2008). The LCG produces and secretes a large amount of proteins and calcium oxalate crystals. Tyrosine-derived  $\beta$ -glucosides from the LCG are converted to protocatechuic acids (PCAs) by RCG  $\beta$ -glucosidase. LCG propenoloxidase (PPO) is activated to phenoloxidase (PO) by compounds from the RCG; then, PO catalyzes the conversion of PCAs to quinones, leading to ootheca hardening and tanning (termed by the PCA pathway) (Courrent et al. 2008; Whitehead 2011). Despite the extraordinary ecological-evolutionary importance of ootheca formation in insects, ootheca structural proteins (OSPs) have never been identified in cockroaches, and thus the molecular mechanism of ootheca formation and its physiological function remain poorly understood.

Recently, we demonstrated that juvenile hormone induces *vitellogenin* (Vg) expression in the fat body and Vg uptake by maturing oocytes during the middle vitellogenesis cycle in *P. americana* (Li et al. 2018; Zhu et al. 2020). Unexpectedly, we found the major RIPA-soluble OSPs as Vgs that are produced by CGs around ootheca laying. We then identified all the major cockroach OSPs, elucidated the detailed molecular mechanism and physiological function of ootheca formation in the cockroach, and further revealed the evolutionary significance of ootheca formation in Polyneoptera. The evo-devo studies highlighted that convergent ootheca formation represents a successful reproductive strategy in Polyneoptera, promoting the radiation of cockroaches, mantids, and locusts during the Triassic-Jurassic period and their establishment in the tropics and subtropics.

## Results

### The LCG Produces Major OSPs around Cockroach Ootheca Laying

The ootheca-laying process in *P. americana* was recorded (fig. 1A and supplementary fig. S2A, Supplementary Material online), confirming that secretions of the large

milk-yellow LCG and the small transparent RCG mix in the genital vestibulum, leading to ootheca formation (Courrent et al. 2008; Whitehead 2011). Since the cockroach OSPs were unknown until today, our first goal was to identify these proteins. After extraction with RIPA lysis buffer, the newly laid ootheca and mature LCG and RCG showed distinct sodium dodecyl sulfate polyacrylamide gel electrophores (SDS-PAGE) protein profiles. Five major ootheca protein bands were excised for in-gel digestion with trypsin, and the trypsin-digested peptides were separated by reversed-phase HPLC followed by mass spectrometry (LC-MS/MS) analysis. Unexpectedly, two major RIPA-soluble proteins were identified as Vgs, with Vg2 being more abundant than Vg1 (supplementary fig. 2B and C, Supplementary Material online).

We then compared the proteomics profiles of newly laid oothecae and mature LCGs and RCGs using urea lysis buffer and LC-MS/MS analysis. The three tissues share 83 common proteins, including proline-rich protein (PRP, GenBank accession number OK335776), Vgs, glucose dehydrogenases, clathrin interactor 1, catalase, and apolipoprotein D. The ootheca and LCG share 24 common proteins, including collagen-like glycine-rich protein (GRP, GenBank accession number OK335777) and laminins, whereas the ootheca and RCG share 15 common proteins, including  $\beta$ -glucosidases (fig. 1B). More than 200 proteins were identified in oothecae, and the top ten were PRP, Vg2, GRP, glucose dehydrogenase 1, Vg1, clathrin interactor 1, laminin subunit  $\beta$ 1, catalase, laminin subunit  $\beta$ 2, and Vg3 (fig. 1C and supplementary fig. S3, Supplementary Material online). Vgs and apolipoproteins are derived from a common ancestor, and they are both mainly produced by the fat body, taken up by maturing oocytes, and later used as nutrients supporting embryogenesis in insects (Babin et al. 1999). However, Vgs are also expressed in other tissues with different physiological functions (Miyazaki et al. 2021; Leipart et al. 2022). PRPs and GRPs are major structural proteins of cell walls in plants, affect the mechanical intensity of plants and cope with various environmental stress (Cassab 1998; Ringli et al. 2001; Mousavi and Hotta 2005; Tseng et al. 2013; Yarawsky et al. 2017; Pinski et al. 2019). PRP and GRP were also found in insects, but their physiological roles have not been investigated (Zhang et al. 2008; Terrapon et al. 2014). Clathrin interactor 1 is a key component involved in clathrin-mediated endocytosis (Mettlen et al. 2018), whereas laminins are critical components of basement membranes (Jayadev and Sherwood 2017). Considering the molecular features of the above proteins, we assume that Vgs, PRP, GRP, clathrin interactor 1, laminins, and apolipoprotein D are the major OSPs.  $\beta$ -Glucosidases, glucose dehydrogenase 1, and laccases are enzymes that are possibly involved in ootheca formation, whereas catalase should be responsible for detoxification by catalyzing  $H_2O_2$  into water and oxygen.

We then examined the spatiotemporal patterns of genes encoding major OSPs using quantitative real-time PCR (qPCR) analysis. PRP (~200-fold higher in the LCG than in the RCG), GRP (~80-fold), and *laminin1* (~40-fold) were most abundantly expressed in the LCG but expressed at much lower levels in the RCG and barely detected in other

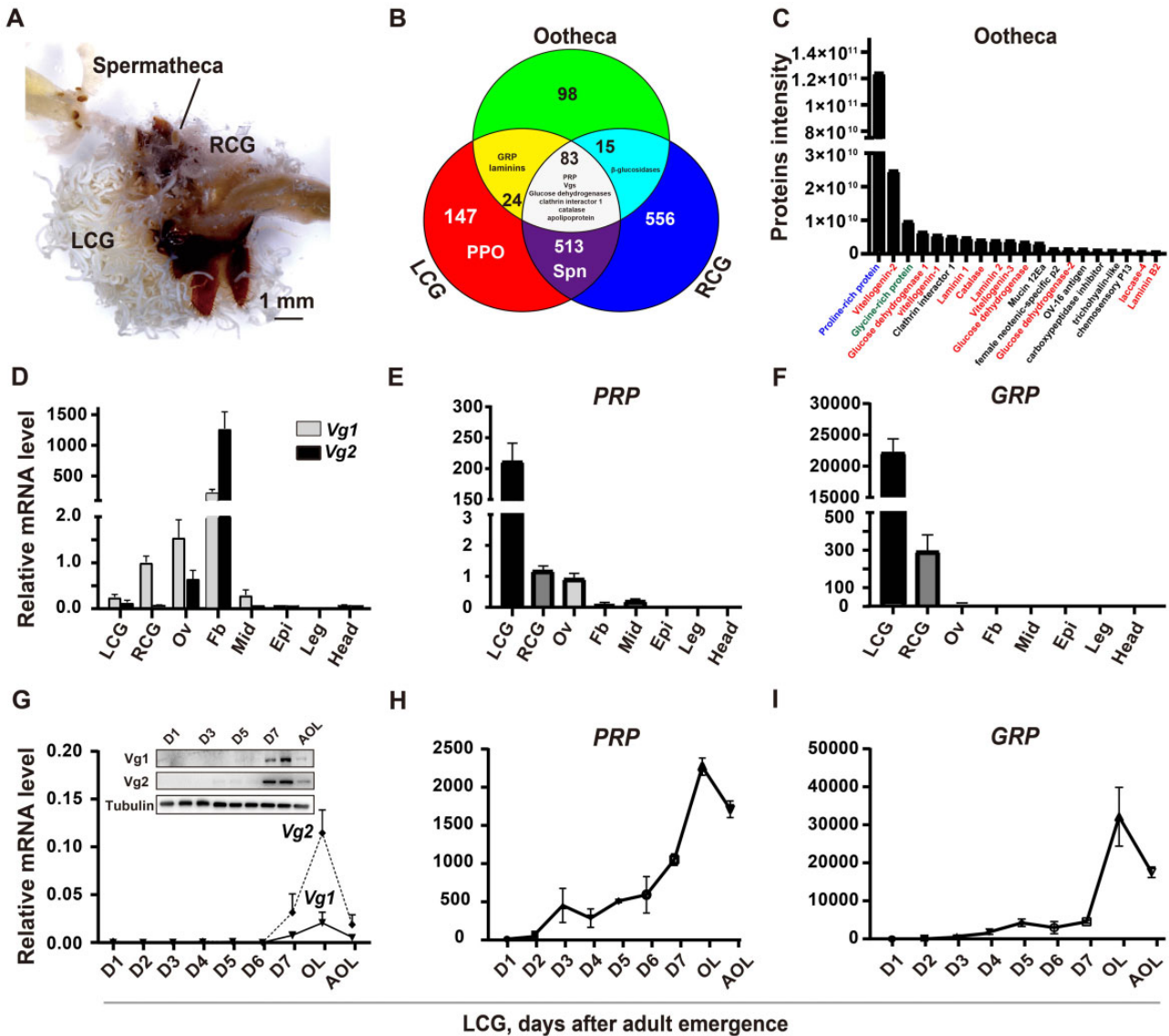


**Fig. 1.** The LCG produces major OSPs around ootheca laying in the cockroach, *Periplaneta americana*. (A) Morphology of an asymmetric pair of CGs during ootheca-laying. (B) Venn diagram of the identified proteins using proteomics data from the newly laid ootheca (green), mature LCG (red), and mature RCG (blue). (C) The intensity ranking of the top 20 OSPs. Red, OSPs shared by the cockroach, mantid, and locust; Blue, OSPs shared by the last two species; Green, species-specific OSPs. (D–I) The spatiotemporal patterns of several major OSP-encoding genes determined using qPCR analysis. Tissue distribution patterns of Vgs (D), PRP (E), and GRP (F). The developmental patterns of Vgs and Vgs (inset) (G), PRP (H), and GRP (I) in the LCG during the first reproductive cycle. Ov, ovary; Fb, fat body; Mid, midgut; Epi, epidermis. D1–D7, day1–day7 PAE; OL, ootheca laying; AOL, after ootheca laying.

tissues. Vgs and *apolipoprotein D* showed the highest expression levels in the fat body, *clathrin interactor 1* was dominantly expressed in the ovary, whereas all the three genes were expressed at low levels in the CGs (fig. 1D–F and supplementary fig. S4A–C, Supplementary Material online). Under the rearing conditions used here, the first reproductive cycle of *P. americana* lasts 7–8 days (Li et al. 2018; Zhu et al. 2020). The mRNA levels of Vgs, PRP, and GRP gradually increased from adult emergence to day 5 postadult emergence (PAE), sharply increased on days 6–7, reached maximal levels during ootheca laying, and dramatically decreased afterwards (fig. 1G–I). We also generated antibodies against Vg1 and Vg2 and measured their developmental profiles. As detected by

Western blots, both Vgs showed developmental patterns similar to their mRNA levels (fig. 1G). The above analyses demonstrate that mainly the LCG produces major OSPs around ootheca laying in the cockroach.

### The LCG and RCG Function Together in Cockroach Ootheca Formation

Since all major OSPs were found in the CGs, we investigated whether OSP gene expression and CG growth have similar developmental profiles. DAPI/phalloidin staining of cryostat sections revealed that the top portions of each CG were composed of an outer layer of secretory cells, an inner layer

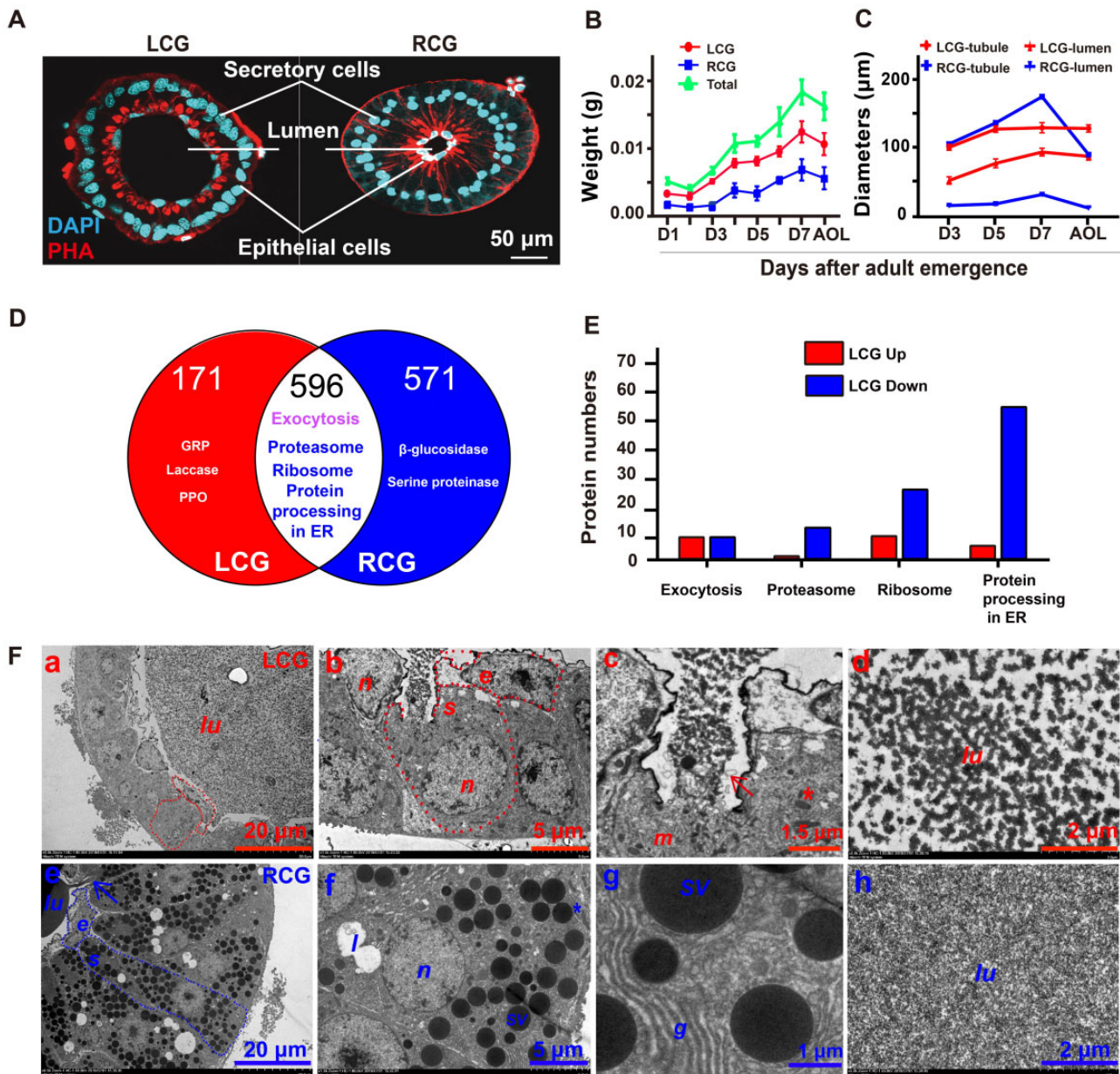


**Fig. 2.** The LCG and RCG function together in ootheca formation in the cockroach, *Periplaneta americana*. (A) Cryostat cross-sections of the LCG and RCG during ootheca-laying followed with DAPI/phalloidin staining. (B, C) The developmental profiles of CGs during the first reproductive cycle. Measurement of CG weight (B) and tubular and luminal diameters (C). (D) Venn diagram of proteins identified from proteomics data of the LCG (red) and RCG (blue). (E) KEGG pathway analysis of enriched proteins between the LCG and RCG as revealed in (D). (F) The subcellular structures of the LCG (a–d) and RCG (e–h) secretory cells captured by TEM. (a) Low-magnification LCG cross-section, showing epidermal cells and secretory cells in the active LCG; (b) details of epidermal cells lining the tubular lumen and exocytosis. (c) Exocytosis. (d) LCG secretions in the lumen. (e) Epidermal cells and secretory cells in the active RCG. (f) Details of a secretory cell with abundant secretory vesicles filled with proteins. (g) Very abundant Golgi (g) and rich secretory vesicles in the cytoplasm. (h) RCG secretions in the lumen. The dashed lines show epithelial cells and secretory cells; e, epithelial cell; s, secretory cell; lu, lumen; n, nucleus; g, Golgi; sv, secretory vesicle; arrows show exocytosis.

of epithelial cells, and a central lumen (fig. 2A). Both the LCG and the RCG grew gradually during the first reproductive cycle, with the LCG being approximately 2-fold heavier than the RCG at most ages. After ootheca laying, the weights of both CGs decreased, exhibiting material transfer from the CGs to the ootheca. The tubular and luminal diameters of both CGs gradually increased during the cycle and decreased after ootheca laying. The tubular diameters of the LCG and RCG were similar, whereas the luminal diameter of the LCG

was much larger than that of the RCG (fig. 2B and C; supplementary fig. S4D and E, Supplementary Material online). Thus, both CGs accomplish sexual maturation by enlarging their tubular sizes and accumulating secretions in the lumen.

To understand how the two CGs coordinately contribute to ootheca formation, we further compared their proteomics data. The LCG and RCG specifically produced 171 and 571 proteins, respectively. Importantly, GRP, PPO, and several laccases were identified in only the LCG, whereas several  $\beta$ -

glucosidases and several serine proteinases were detected solely in the RCG (fig. 2D). Moreover, two CGs shared 596 proteins, many of which are involved in four pathways. Quantitative analysis showed that proteins in the exocytosis pathway were highly detected in both CGs, whereas proteins in the proteasome pathway, the ribosome pathway, and protein processing in the endoplasmic reticulum pathway were more abundant in the RCG (fig. 2E and supplementary fig. S4F, Supplementary Material online). We then examined the subcellular structure of secretory cells in each CG by using transmission electron microscopy (TEM). RCG secretory cells are much larger than LCG secretory cells. Endoplasmic reticulum, Golgi complexes, mitochondria, and secretory vesicles are abundant in the secretory cells of both CGs. Exocytosis-mediated secretions in the LCG secretory cells and the central lumen were frequently observed, whereas numerous dark secretory vesicles were present in RCG secretory cells (fig. 2F). The proteomics data and morphological observations suggest that the two CGs play both similar and differential roles in ootheca formation, the specified LCG mainly produces OSPs and has a very strong secretory capability, whereas significant protein synthesis, processing, and degradation occur in the RCG.

### OSP Sclerotization and Melanization Leading to Cockroach Ootheca Formation

To complement the proteomics analysis, we performed metabolomics analysis to better understand the underlying molecular mechanism of ootheca formation in *P. americana*. Up to 1,665 known metabolites were detected in the LCG, RCG, and ootheca, with 1,410 common metabolites observed in all three tissues (fig. 3A). Quantitatively, principal component analysis and heatmap analysis of the metabolites revealed that the LCG and RCG closely clustered together but were separated from the ootheca (fig. 3B and B'). KEGG analysis of the metabolites revealed three major pathways. The phenylalanine and tyrosine metabolism pathway involved in the early steps of sclerotization and melanization was significantly enriched in the LCG. The pathway of calcium chemicals for the production of calcium oxalate crystals was detected in all three tissues, whereas the sclerotization and melanization pathway was enriched in the ootheca and LCG (fig. 3C). Notably, a number of chemical compounds were identified for OSP sclerotization and melanization, including phenylalanine, tyrosine, tyramine,  $\beta$ -glucoside, 3,4-dihydroxybenzoic acid, p-quinone, 3,4-dihydroxyphenylalanine (DOPA), dopamine, dopachrome, indole-5,6-quinone 2-carboxylic acid, and 5,6-dihydroxyindole (fig. 3D), showing that OSPs undergo sclerotization and melanization leading to cockroach ootheca formation.

Combining the proteomics and metabolomics data, we propose a model of OSP sclerotization and melanization involved in ootheca formation in *P. americana*. Mainly in the LCG, phenylalanine is first dehydroxylated to tyrosine. Tyrosine is catalytically converted to a variety of quinones and melanochromes in the genital vestibulum, causing OSP sclerotization and melanization via two cooperative pathways: the PCA pathway and the DOPA and dopamine

pathway (the dopachrome and dopaminechrome subpathway) (fig. 3D and supplementary fig. S5, Supplementary Material online). The PCA pathway has been studied only in the cockroach ootheca (Bell and Adiyodi 1981; Courrent et al. 2008; Whitehead 2011), the DOPA and dopamine pathway has been extensively examined in the cuticle (Andersen 2010; Dittmer and Kanost 2010; Willis 2010; Noh et al. 2016; Sugumaran and Barek 2016), which is shown here functionally important for ootheca formation for the first time. In the PCA pathway mainly caused by the LCG, tyrosine is decarboxylated to tyramine, which undergoes a series of chemical reactions and is converted to a variety of  $\beta$ -glucosides. RCG  $\beta$ -glucosidases convert  $\beta$ -glucosides to PCAs, and the remaining glucose is metabolized by glucose dehydrogenases. LCG PPO is activated to PO, and this activation can be inhibited by some serpins from both CGs. Under the activation of LCG laccases and PO, PCAs are converted to quinones, leading to sclerotization. In the dopachrome and dopaminechrome subpathway mainly caused by the RCG, tyrosine is hydroxylated to DOPA and further decarboxylated to dopamine. Both DOPA and dopamine undergo decarboxylation to generate dopaquinone and dopamine-quinone, which are converted to the corresponding dopachrome and dopaminechrome. Quinones cause sclerotization, whereas melanochrome polymerization leads to melanization. Notably,  $\beta$ -glucosidases, PO, and laccase are key enzymes in the two pathways. The enlarged LCG is specified, produces a large amount of OSPs and several key enzymes in the two pathways, whereas the most important enzymes in the RCG are  $\beta$ -glucosidases. The asymmetric CGs guarantee effective OSP sclerotization and melanization caused by the two cooperative pathways.

### OSP Sclerotization and Melanization Prevent Egg Water Loss and Maintain Embryo Viability in the Cockroach at Warm and Dry Conditions

To explore the roles of OSP sclerotization and melanization in ootheca formation, we injected adult female cockroaches with double-stranded RNA (dsRNA) to silence the expression of *PRP* and *GRP*, with small interfering RNA (siRNA) to reduce the expression of *Vgs* and *laccase 2*, and with the chemical inhibitors conduritol B epoxide, lanthanum (III) chloride heptahydrate, PTU, and MG132 to inhibit the activities of  $\beta$ -glucosidases, calcium-mediated exocytosis, PO, and the proteasome, respectively. Phenotypic changes in the thickness, weight, and color of the ootheca were then observed. The RNAi efficiency of *PRP*, *GRP*, *Vgs*, and *laccase 2* was approximately 90% (fig. 4A). RNAi knockdown of *PRP* reduced about half of ootheca thickness, and it also reduced ootheca weight and caused ootheca a lighter color. RNAi knockdown of *GRP* or *Vgs* reduced ootheca thickness and weight but did not affect ootheca color. Injections with lanthanum (III) chloride heptahydrate not only reduced ootheca thickness and weight but also caused it a much lighter color. Differently, RNAi knockdown of *laccase 2* and injections with conduritol B epoxide and PTU caused a lighter color but had no effect on ootheca thickness and weight, and MG132 had little effects (fig. 4A–D and supplementary fig. S6A–E,

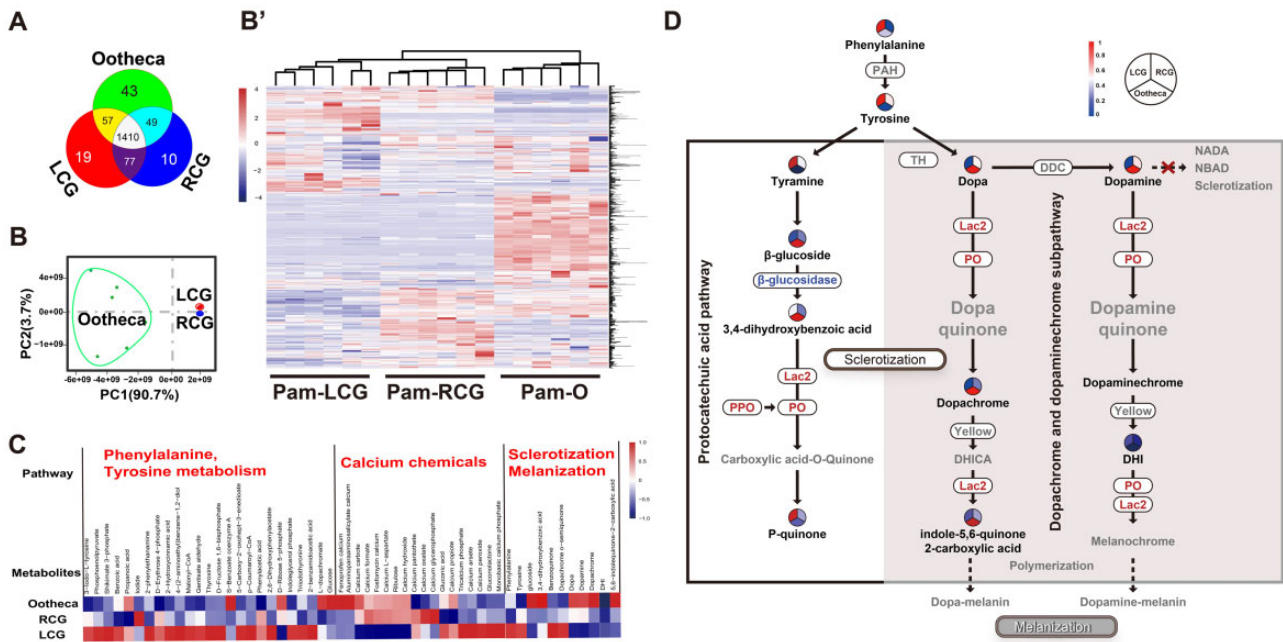


**Fig. 3.** OSPs undergo sclerotization and melanization leading to ootheca formation in the cockroach, *Periplaneta americana*. (A) Venn diagram showing the numbers of known metabolites identified from metabolomics data among the LCG, RCG, and ootheca. (B, B') Principal component analysis (B) and heatmap analysis (B') showing the abundance patterns of the identified metabolites. (C) KEGG analysis of key metabolic pathways and heatmap of the mapped metabolites. (D) A model of the molecular mechanism of ootheca formation in *P. americana*: OSPs undergo sclerotization and melanization for ootheca formation. The black border with the solid line indicates the PCA pathway, and the border with the gray line under a background indicates the dopachrome and dopaminechrome subpathway. Quinones cause sclerotization, whereas melanochrome polymerization leads to melanization. All proteins are shown in boxes (blue for RCG; red for LCG); undetectable metabolites or proteins are indicated in gray. Circular heatmaps represent the expression level of metabolites of interest among the LCG, the RCG, and ootheca. PAH, phenylalanine hydroxylase; TH, tyrosine hydroxylase; DDC, dopa decarboxylase; PPO, polyphenoloxidase; PO, phenoloxidase; Lac2, Laccase 2; Yellow, dopachrome conversion enzyme; DHICA, 5,6-dihydroxyindole-2-carboxylic acid; DHI, 5,6-dihydroxyindole; NADA, *N*-acetyldopamine; NBAD, *N*- $\beta$ -alanyldopamine.

Supplementary Material online). The proteomics, ultrastructural, and functional analyses together reveal that the structurally and functionally distinct LCG and RCG coordinate ootheca formation. The functional analyses confirmed the importance of OSP sclerotization and melanization in ootheca formation caused by the two cooperative pathways (fig. 3D and supplementary fig. S5, Supplementary Material online).

The cockroach rearing conditions used in our laboratory are 37 °C and 70% relative humidity (RH), and a temperature higher than 37 °C or a humidity lower than 70% significantly decreases the egg hatching rate (Li et al. 2018; Zhu et al. 2020). We therefore examined whether the ootheca was responsible for preventing water loss from eggs and maintaining embryo viability at a relatively high temperature (37 °C) and 70% RH in the cockroach *P. americana*. As expected, at 70% RH, water loss from the oothecae gradually increased with a temperature change from 30 to 37 °C and further to 44 °C (supplementary fig. S5F, Supplementary Material online). We then tested whether the major OSPs (including PRP, Vgs, and GRP) and  $\beta$ -glucosidases impacted water retention in the oothecae under normal laboratory rearing conditions. Either RNAi knockdown of the OSP-encoding genes or injection with the  $\beta$ -glucosidase inhibitor condiritol B epoxide, which was

able to disturb OSP sclerotization and melanization for ootheca formation, increased water loss of the oothecae, with RNAi knockdown of *GRP* showing strongest phenotypic defects. Compared with the controls in which less than 5% of ootheca water was lost seven days after ootheca laying, water loss rate increased to approximately 40% upon *GRP* knockdown (fig. 4E and F). Moreover, RNAi knockdown of *GRP* resulted in 40% and 60% distorted oothecae one day and seven days after ootheca laying, showing much stronger effects on ootheca distortion than other treatments. Importantly, the egg hatching rate from oothecae was about 40% in control groups, whereas no egg hatching was observed in the RNAi experimental groups, showing the crucial role of ootheca in water retention (fig. 4G and H; supplementary fig. S6I, Supplementary Material online). In addition, we examined whether PRP prevents water loss at 37 °C and 100% RH by RNAi knockdown of *PRP*. Indeed, compared with 37 °C and 70% RH, the higher humidity dramatically reduced water loss rate and distorted ootheca rate in both control and experimental groups, confirming the importance of ootheca formation for water retention in dry conditions (supplementary fig. S6G and I, Supplementary Material online). The water loss experiment shows that OSP sclerotization and

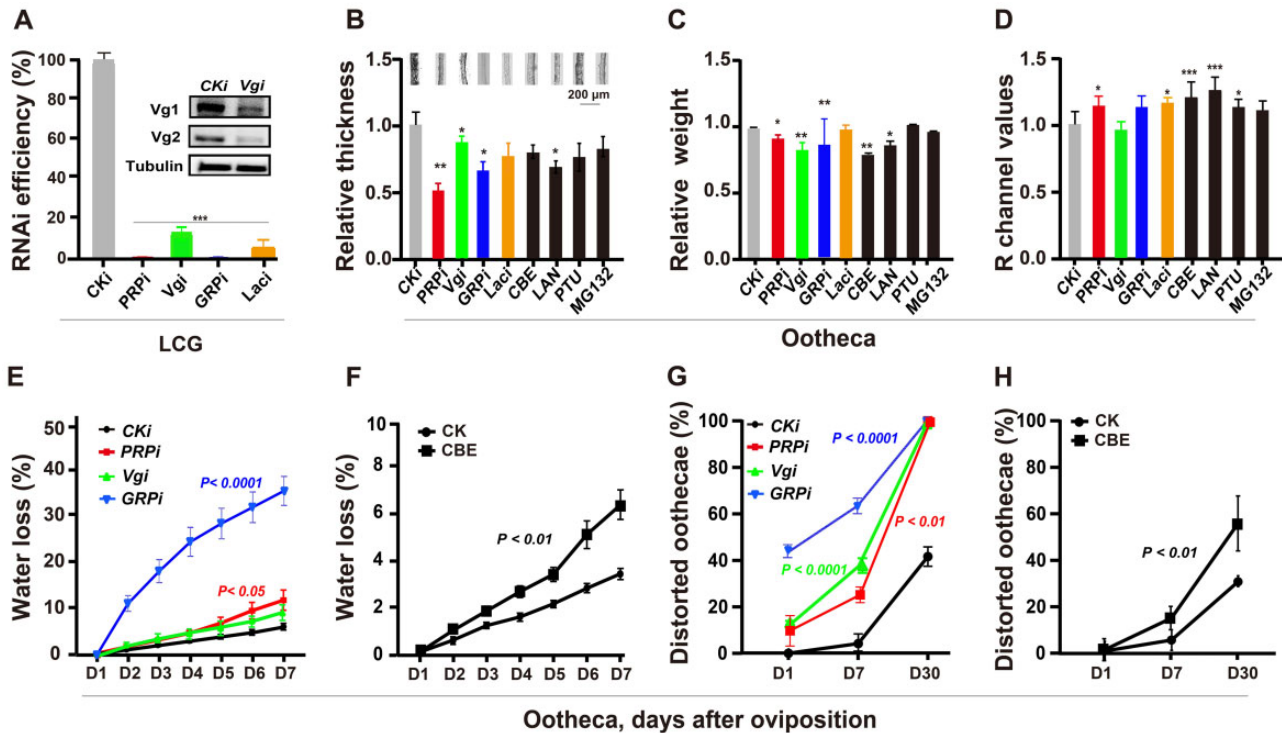


**FIG. 4.** OSP sclerotization and melanization prevent egg water loss and maintain embryo viability in the cockroach, *Periplaneta americana*, at warm and dry conditions. (A) RNAi efficiency of *PRP*, *Vgs*, *GRP*, and *laccase 2* in the LCG as detected by qPCR analysis. The inset shows Western blotting of *Vg1* and *Vg2*. (B–D) The effects of RNAi of four OSP-encoding genes and the injection of four chemical inhibitors on ootheca thickness (B), weight (C), and color (channel value) (D). LAN,  $Ca^{2+}$  inhibitor; MG-132, proteome inhibitor; CBE,  $\beta$ -glucosidase inhibitor; PTU, PPO inhibitor. (E, F) The effects of RNAi of *PRP*, *Vg*, and *GRP* (E) and injection of CBE (F) on ootheca water retention. (G, H) The efficiency of RNAi of *PRP*, *Vg*, and *GRP* (G) and injection of CBE (H) on causing ootheca distortion ( $N = 25$ ). To make it easy to follow, three colors represent the three key OSPs including *PRP* (red), *Vgs* (green), and *GRP* (blue).

melanization prevent eggs from losing water and thus effectively maintain embryo viability at warm and dry conditions, shedding light on why cockroaches thrive in the tropics and subtropics but prefer living in wet places, such as sewer.

### Ootheca Formation Convergenly Evolved in Polyneoptera

A recent phylogenetic analysis suggests that the last common ancestors of Polyneoptera were terrestrial. However, as a representative of the earliest insect radiation, Polyneoptera is characterized by a wide spectrum of different lifestyles, habitat preferences, reproductive strategies, social behaviors, and body shapes. Physiological and behavioral specializations might have undergone adaptation multiple times within Polyneoptera, showing numerous events of convergent evolution (Wipfler et al. 2019). We then employed morphological, proteomics, and metabolomics analyses to compare the mechanisms underlying ootheca formation in the cockroach *P. americana*, the giant Asian mantid, *Hierodula patellifera*, and the migratory locust, *Locusta migratoria*. The field cricket, *Gryllus testaceus*, which belongs to Orthoptera but does not produce oothecae, was used as a negative control.

The morphological features of oothecae and CGs were examined using light microscopy and scanning electron microscopy (SEM). The surfaces of all three types of oothecae are composed of hexagonal or hexagon-like skeleton units.

The hexagonal skeleton units of the cockroach ootheca are thick and covered by numerous dotted materials; those of the mantid ootheca are thick but smooth, whereas those of the grasshopper ootheca are thin and smooth (fig. 5A). Meanwhile, the CGs in both the cockroach and the mantid are asymmetric, with the LCG being much larger than the RCCG, whereas the CGs in both the locust and the cricket are symmetric, again strengthening the conclusion that asymmetric CGs are responsible for efficient ootheca formation in dictyopterans (supplementary fig. S8, Supplementary Material online).

In proteomics analysis, 15 common proteins, including *Vgs*, apolipoprotein D, laccases, laminins, and serpins, were identified among the three types of oothecae. The ootheca proteomics data show that *Vgs*, apolipoprotein D, and laminins are common OSPs in the relatively distantly related dictyopterans and locusts, providing strong evidence for convergent evolution of ootheca formation in Polyneoptera. Meanwhile, laccases and PO are enzymes involved in OSP sclerotization and melanization, suggesting both the PCA pathway and the dopachrome and dopaminechrome sub-pathway are employed for ootheca formation in these insects. Significantly, *Vgs* are among the top OSPs in the locust and cockroach, but not in the mantid. *PRP* ranked as the No. 1 OSP in both the cockroach and the mantid but was undetectable in the locust. *GRP* was identified only in the

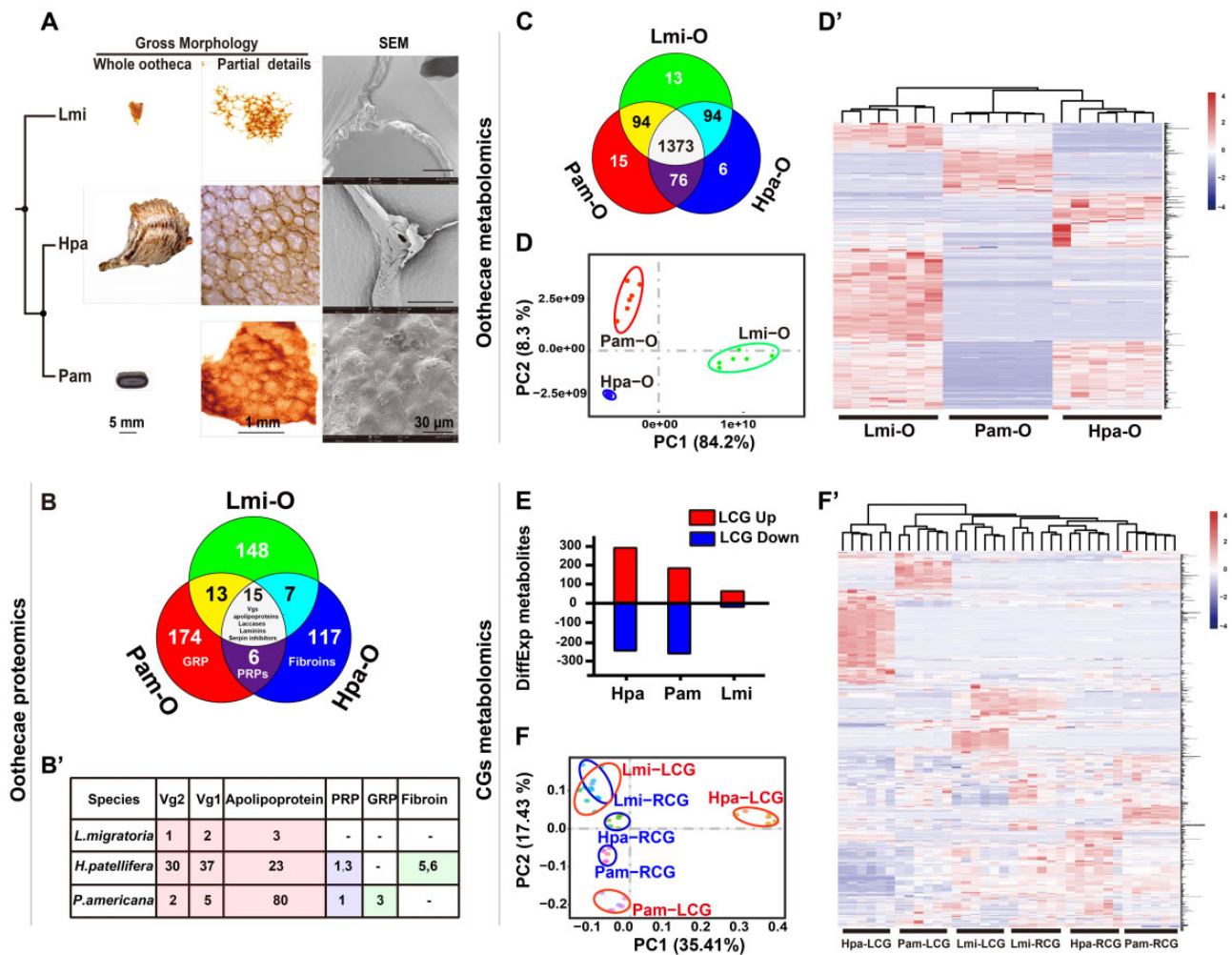


**Fig. 5.** Convergent evolution of ootheca formation in Polyneoptera. (A) Comparison of the ootheca morphological features of the locust *Locusta migratoria* (Lmi), mantid *Hierodula patellifera* (Hpa), and cockroach *Periplaneta americana* (Pam) captured by light microscopy or SEM. (B) Venn diagram of proteins in fresh oothecae of the three species. (B') Ranking of major OSPs in the oothecae of the three species. The details were shown in [supplementary table S1, Supplementary Material online](#). (C) Venn diagram showing the numbers of annotated metabolites in the oothecae of the three species. (D, D') Principal component analysis of annotated metabolites (D) and heatmap showing the abundance patterns of annotated metabolites (D') in the oothecae of the three species. (E) Numbers of differentially expressed metabolites ( $P$  value of  $t$ -test  $< 0.05$  and  $VIP \geq 1$ ) between the LCG and RCG within the three species. (F, F') Principal component analysis of known metabolites (F) and heatmap showing the abundance patterns of annotated metabolites (F') in the LCG and RCG of the three species.

cockroach, whereas coiled-coil fibroins were unique to the mantid, showing that cockroach and mantid independently developed some of their own OSPs during evolution (fig. 5B and B'; supplementary fig. S7A and B, fig. S8, and table S1, Supplementary Material online). In addition, Yellow, a laccase 2-like dopachrome-conversion enzymes, is also found in the mantid CGs by proteomics (Matsuoka and Monteiro 2018) (supplementary table S1, Supplementary Material online).

Metabolomics analysis identified a total of 1,670 known metabolites from the CGs and oothecae of selected representative insect species. Similar to the metabolomic profile in the cockroach, close clustering of the LCG and RCG and their separation from the ootheca were also observed in the locust and mantid (supplementary fig. S7C and D, Supplementary Material online). The three types of oothecae shared 1,373 metabolites, including the chemical compounds involved in both the PCA pathway and the dopachrome and

dopaminechrome subpathway (fig. 5C). To quantitatively determine the variability in metabolites among the three types of oothecae, we further performed principal component analysis and heatmap analysis. The three types of oothecae were separated from one another, with a closer relationship between the cockroach and mantid oothecae (fig. 5D and D'). We then compared the differentially expressed metabolites between the CG pairs of the three insect species. Up to 500 differentially expressed metabolites were found between the asymmetric LCG and RCG in the mantid, similar to the pattern in the cockroach. However, only a few metabolites were differentially expressed between the locust CG pairs (fig. 5E). The abundances of known metabolites in the LCGs of the cockroach and mantid were separated from those in the locust LCG and all RCGs, with the mantid LCG showing a remote relationship with the others (fig. 5F and F'). The metabolomics data revealed that in dictyopterans, the LCG



had a greater diversification rate than the RCG, and the mantid LCG specialized even faster than the cockroach LCG, highlighting the importance of asymmetric CGs. In addition, when the cricket CGs were analyzed together, they showed very different metabolomics profiles from the CGs of the other three species (supplementary fig. S7E and E', Supplementary Material online). Thus, polyneopterans utilize both the PCA pathway and the dopachrome and dopamine-chrome subpathway for OSP sclerotization and melanization. However, the mantid and locust show a preference for the PCA pathway, whereas the cockroach shows a preference for the dopachrome and dopamine-chrome subpathway (supplementary fig. S8, Supplementary Material online).

The composite data demonstrate the convergent evolution of ootheca formation in Polyneoptera, which was adapted as a successful reproductive strategy that promoted the radiation and establishment of cockroaches, mantids, and locusts (fig. 6 and supplementary fig. S8, Supplementary Material online).

## Discussion

### OSP Sclerotization and Melanization for Ootheca Formation through Two Cooperative Pathways

To understand the molecular mechanism of ootheca formation in the cockroach, we first identified the major OSPs in *P. americana* using proteomics. Similar to our findings that PRP and GRP are major cockroach OSPs, they are major structural proteins in plant cell walls (John and Keller 1995; Ringli et al. 2001; Mousavi and Hotta 2005; Hunt et al. 2017), showing independent adaptation of these two types of proteins as protecting structural components in both plants and insects. In plants, PRPs and GRPs bind to a wide range of proteins and thus form protein complexes, they also bind to and precipitate polyphenols, quinones, and melanochromes, and thus form insoluble complexes (Cassab 1998; Tseng et al. 2013; Yarawsky et al. 2017; Pinski et al. 2019). Thus, PRRs, GRPs, and their associated proteins might undergo sclerotization and melanization for ootheca formation in insects through the two cooperative pathways. It was surprising to identify Vgs as major OSPs, since Vgs primarily play nutritional roles in embryogenesis (Raikhel 2005). As extracted with RIPA lysis buffer, the newly laid ootheca and fat body tissues at the vitellogenesis stage exhibit very similar SDS-PAGE protein profiles. Interestingly, Vgs and apolipoproteins are RIPA-soluble, implying that they do not tightly bind to PRPs and GRPs that form strong protein complex. Nevertheless, Vg expression in the fat body and in the LCG peak during middle vitellogenesis and ootheca laying, respectively. The distinct spatiotemporal patterns of Vgs are in agreement with their different roles in the embryo and ootheca (Zhu et al. 2020). Since Vgs and apolipoprotein D are derived from a common ancestor (Babin et al. 1999), it will be interesting to further examine whether similar changes of DNA regulatory elements and/or transcriptional regulation mechanisms simultaneously occurred in their encoding genes. Importantly, RNAi knockdown of *PRP*, *GRP*, and *Vgs* reduced ootheca thickness and increased ootheca water loss,

confirming their physiological roles as major OSPs in the cockroach.

Proteomics and metabolomics in *P. americana* together revealed a number of enzymes and chemical compounds involved in OSP sclerotization and melanization by quinones or melanochromes through two cooperative pathways: the PCA pathway and the dopachrome and dopamine-chrome subpathway (fig. 3D and supplementary fig. S5, Supplementary Material online). The tanning and hardening processes of the cuticle and ootheca differ as follows. 1) Laccases are important for both the ootheca and the cuticle, but PO is not required for the cuticle. 2) The PCA pathway was detected only in the ootheca. 3) In the DOPA and dopamine pathway, the dopachrome and dopamine-chrome subpathway is functionally important for melanization in both the ootheca and the cuticle. 4) In the DOPA and dopamine pathway, the *N*-acetyldopamine and *N*- $\beta$ -alanyldopamine subpathway is required for melanization in the cuticle but not in the ootheca.

We suppose that asymmetric CGs enable effective OSP sclerotization and melanization leading to ootheca formation in *P. americana* (fig. 3D and supplementary fig. S5, Supplementary Material online). The asymmetric CGs play both similar and differential roles in ootheca formation. Without the mixture of the secretions from both CGs in the genital vestibulum, no quinones or melanochromes can be produced, no OSP sclerotization or melanization occurs, and no ootheca forms. This elegant cooperation between the two CGs causes effective OSP sclerotization and melanization and thus ootheca formation. The enlarged LCG produces all major OSPs and a big number of enzymes, whereas the RCG should have other roles besides producing  $\beta$ -glucosidases since significant protein synthesis, processing, and degradation occur in this tissue. For example, (Z)-docos-13-enamide is abundantly detected in the RCG and likely functions like quinones or melanochromes. Another interesting insect case is that bombardier beetles use a rapid series of discrete explosions, producing a hot, pulsed, quinone-based defensive spray with both reservoir and reaction chambers (Arndt et al. 2015). Related studies in these insects might have a bright future in biomechanics and bionics.

### Convergent Evolution of Ootheca Formation in Polyneoptera

As inferred from the insect phylogenetic tree, the common ancestor of dictyopterans lived approximately 231 Ma. Although the divergence time of locusts and crickets in Orthoptera was approximately 203 Ma, that of cockroaches and mantids in Dictyoptera was approximately 197 Ma (Misof et al. 2014) (supplementary fig. S1, Supplementary Material online). Notably, all these important evolutionary events occurred during the last half of the Triassic period (250–200 Ma) and the beginning of the Jurassic period (205–144 Ma), which coincided with the period of the fourth mass extinction under high land surface temperatures and comparatively low moistures (Tanner et al. 2004). Therefore, the independent ootheca formation in Polyneoptera might have been due to geologic events on Earth during the Triassic-

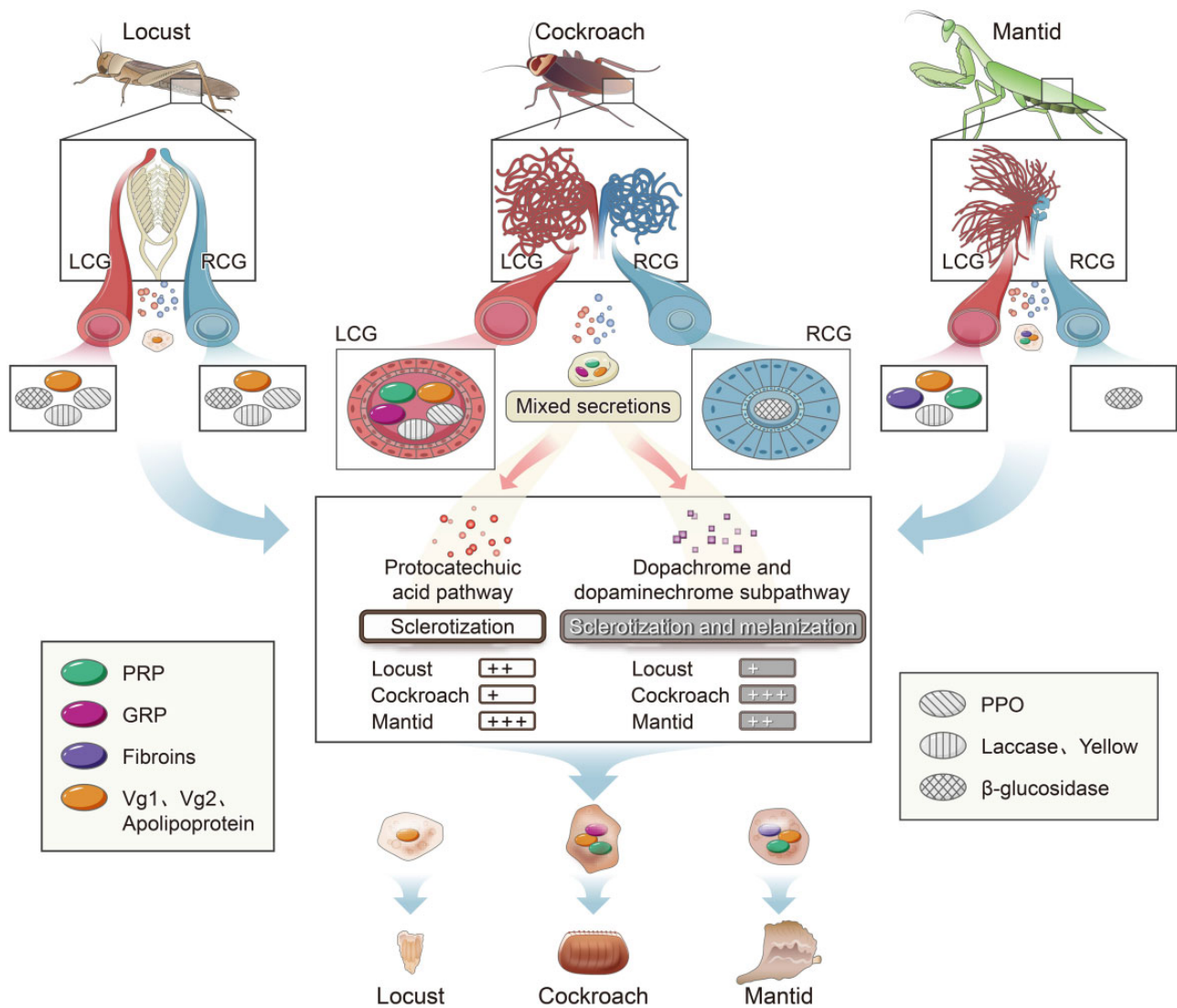


**FIG. 6.** The evo–devo pattern underlying ootheca formation in Polyneoptera. Comparison of OSP sclerotization and melanization for ootheca formation among the cockroach *Periplaneta americana*, the mantid *Hierodula patellifera*, and the locust *Locusta migratoria*. Common features of ootheca formation in Polyneoptera: both the PCA pathway and the dopachrome and dopaminechrome subpathway commonly exist in the CGs. Ootheca is likely a specialized approach for egg packaging. Convergent evolution of ootheca formation in Polyneoptera: both Vgs and apolipoprotein D are expressed in the CGs and used for as OSPs for ootheca formation, providing the strongest evidence of convergent evolution of ootheca formation in Polyneoptera. Common features of ootheca formation within Dictyoptera: the asymmetric CGs in dictyopterans that effectively produce oothecae; dictyopterans share PRP as the major OSP. Further evolution of ootheca formation within Dictyoptera: cockroaches and mantids have developed GRP and fibroins as distinct OSPs.

Jurassic period, that is, warm and dry environmental conditions, resulting in convergent adaptation as a reproductive strategy in Polyneoptera.

The earliest fossil evidence of dictyopteran oothecae (237–227 Ma. Late Triassic, Cariglino et al. 2020) is consistent with the existence of crown-Dictyoptera inferred by molecular data (Misof et al. 2014), and supports the single origin of dictyopteran ootheca. However, Dictyoptera has a long fossil record—roachoid insects were already present 300 Ma in the Carboniferous forests. Their relationships to crown-group Dictyoptera remain unresolved, so these stem-group dictyopterans are usually not included in the insect systematics (Grimaldi and Engel 2005). These early

fossil roachoids possessed a very long and prominent ovipositor, indicating that they were not able to produce oothecae (Hörnig et al. 2018). These fossil records strongly support that oothecae evolved in the ancestor of crown-Dictyoptera independently. Oothecae also evolved in other polyneopterans, including crickets (Orthoptera: Ensifera), gladiators (Mantophasmatodea), and a single species of stick insects (Phasmatodea) (Gillott 2005; Goldberg et al. 2015; Küpper et al. 2019), as well as a few species of holometabolous insects (Huang et al. 2006; Flowers and Chaboo 2015; Malek et al. 2019). The analyses strongly suggest that insect ootheca evolved multiple times independently and convergently based on the parsimony principle (Crisi

1982; Coelho et al. 2019), although one is not able to completely deny the possibility of the single origin of ootheca in the last common ancestor of “orthopteroids.”

Our study reveals that the cockroach ootheca contains a variety of proteins, and only some of them (such as Vgs and apolipoproteins) have homology in the locust ootheca. Homologous Vgs and apolipoproteins shared by locust and dictyopteran ootheca are the strongest molecular evidences for the convergent evolution of ootheca formation independently arose in the relatively distantly related dictyopterans and locusts. Meanwhile, diverse OSPs (such as PRP, GRP, and fibroins) suggest different molecular mechanism of ootheca formation between dictyopterans and locusts. Although dictyopterans share PRP as the most abundant OSP, cockroaches and mantids independently developed GRP and fibroins as distinct OSPs, respectively, likely due to a functionally convergent evolution. Lacking PRP and GRP that form tightly insoluble complex (Cassab 1998; Tseng et al. 2013; Yarowsky et al. 2017; Pinski et al. 2019), Vgs and apolipoproteins alone in locusts should not be able to yield an ootheca that are as strong as the dictyopterans. In addition, since PRPs and GRPs are the most abundant structural proteins in plant cell wall (Tseng et al. 2013), it is likely that using PRPs and GRPs as structural proteins in plant cell walls and insect oothecae result from a convergent evolution.

The CG is a type of specialized female accessory gland that produces substances for packaging eggs, adhering the eggs to a substrate, and providing a protective coating over the eggs. Since CGs are responsible for ootheca formation, ootheca could be a specialized approach for egg packaging. For example, the mosquito eggshell (or chorion) is produced by female accessory glands, and chorion proteins also undergo sclerotization and melanization through the DOPA and dopamine pathway (Li and Christensen 1993; Marinotti et al. 2014). Proteomics and metabolomics in this study together reveal that dictyopterans and locusts independently employed OSP sclerotization and melanization for ootheca formation. Notably, in both the cockroach and the mantid, the enlarged LCG produces a big amount of OSPs and several important enzymes leading to extremely efficient OSP sclerotization and melanization, and the resulting thick ootheca covers numerous eggs in a highly ordered arrangement. In conclusion, ootheca formation is one of the numerous events of convergent evolution in Polyneoptera (Wipfler et al. 2019) (fig. 6 and supplementary fig. S8, Supplementary Material online).

### Convergent Adaptation of Ootheca Formation as a Reproductive Strategy in Polyneoptera

The common ancestor of crown-dictyopterans (cockroaches and mantids) and that of orthopterans (locusts and crickets) occurred during the late Triassic or the early Jurassic period, which coincided with the comparatively high temperatures and low moistures in the land surface caused by the fourth mass extinction. Overall, warm and dry conditions should be important environmental causes of ootheca formation, as supported by fossil records (Tanner et al. 2004; Cariglino et al. 2020).

Since landing approximately 480 Ma, insects live in various terrestrial environments, evolved and retained different morphological features. Due to the mass extinction during the Triassic-Jurassic period, new ecosystems were built by the so-called modern groups, including most extant insect families (Misof et al. 2014; Benton 2016). Polyneoptera, one of the major winged lineages, comprises approximately 40,000 extant species belonging to ten orders, whereas Blattodea (5,000 species), Mantodea (2,200 species), and Orthoptera (13,300 species in total, including 5,000 locust species) account for more than one-half of the polyneopteran biodiversity (Misof et al. 2014; Wipfler et al. 2019), suggesting their successful adaptation on Earth. Both the ootheca and the cuticle are waterproof, and the water retardation capacity of the ootheca is much stronger than that of the cuticle in cockroaches (Young et al. 2000; Mullins et al. 2002; Howard and Blomquist 2005; Chen et al. 2020). As supported by fossil records during the Late Triassic (Tanner et al. 2004; Cariglino et al. 2020), ootheca provides an advantageous strategy for protection against desiccation in warm and dry conditions. Importantly, disturbing OSP sclerotization and melanization significantly increased water loss of the oothecae and caused ootheca distortion. We suppose that one of the original roles of ootheca was to prevent water loss from the eggs and thus maintain embryo viability at relatively high temperatures and low moistures during the Triassic-Jurassic period. Concomitantly, the ootheca protects the eggs from predators, parasitoids, pathogens, and other environmental sources of injury. In summary, ootheca formation is a convergent reproductive strategy that promoted the biodiversity in Polyneoptera.

From the evo–devo perspective, we inferred the evolutionary history of ootheca formation in Polyneoptera (fig. 6 and supplementary fig. S8, Supplementary Material online). During the Triassic-Jurassic period, the common ancestor of crown-dictyopterans evolved oothecae depending on OSP sclerotization and melanization, which could prevent water loss from eggs. The asymmetric CG pairs in dictyopterans might have resulted in significant ootheca formation that prevents eggs from losing water at warm and dry conditions and thus effectively maintain embryo viability. As an adaptive reproductive strategy, ootheca formation promoted polyneopteran radiation during the Triassic-Jurassic period, shedding light on why cockroaches, mantids, and locusts currently thrive in tropics and subtropics. This study demonstrated the ecological-evolutionary significance of ootheca formation in Polyneoptera.

## Materials and Methods

### Insects

The American cockroach *P. americana* was raised under laboratory conditions as previously described (Li et al. 2018; Zhu et al. 2020). The cockroaches were maintained in a plastic box (45 cm × 32 cm × 27 cm) with enough ddH<sub>2</sub>O and sterile mouse chow diet with 1.06% calcium and 0.99% phosphate under laboratory conditions at 28 °C and 70–80% RH under a 12:12 h (light: dark) photoperiod. The giant Asian mantid

*H. patellifera*, the migratory locust *L. migratoria*, and the field cricket *G. testaceus* were bought and raised in the laboratory for a short period before use. *Hierodula patellifera* insect was fed with cockroach larvae. *Locusta migratoria* insects were fed with fresh weeds in a plastic cage with soil. *Gryllus testaceus* insects were reared at 25 °C with a commercial dog food and water.

## Morphological Feature Examination

### Light Microscopy

Images of the insects, oothecae, and tissues were captured with a Nikon DS-Ri2 camera and analyzed with a Nikon SMZ25 microscope (Nikon, Japan) (Zhu et al. 2020).

### Confocal Microscopy

Histological investigation of the CGs and oothecae was validated by DAPI/phalloidin staining of cryostat sections as previously described (Zhu et al. 2020). The images were taken by an Olympus FluoView FV3000 confocal microscope and analyzed with FV31S-SW software (Olympus, Japan) (Zhu et al. 2020).

### Scanning Electron Microscopy

The dissected CGs and fresh oothecae were washed with phosphate-buffered saline and dried in a high-vacuum environment. The samples were adhered onto stubs with double-sided tape, and photographs were taken with a JEOL SEM at 5 kV (JSM-6360LV) (JEOL, Japan).

### Transmission Electron Microscopy

The CGs were dissected and processed for TEM analysis as previously described, and the ultrastructure of CG cells was visualized and captured using an HT7700 transmission electron microscope (Hitachi, Japan) (Tian et al. 2013).

## Treatments

### Inhibitor Application

A female adult of *P. americana* was injected with 2  $\mu$ l inhibitor solution three times on days 4, 6, and 8 PAE. The chemical inhibitors included conduritol B epoxide (10 mM, catalog no. HY-100944/CS-6107, MedChem Express LLC), lanthanum (III) chloride heptahydrate (10 mM, catalog no. CSN23827, CSNpharm), PTU (saturated liquid in ddH<sub>2</sub>O, generously donated by Dr Erjun Ling), and MG132, a proteasome inhibitor (1 mM, dissolved in DMSO; Sigma–Aldrich).

### RNAi

As found in the preliminary results, dsRNA worked properly for RNAi knockdown of *PRP* and *GRP*, whereas siRNA but not dsRNA resulted in highly efficient RNAi knockdown of *Vgs* and *laccase 2* in the CGs (Li et al. 2018; Zhu et al. 2020). The dsRNAs of *PRP*, *Vgs*, *GRP*, *Lac2*, and *GFP* (control) were synthesized via in vitro transcription using a T7 RiboMAX Express RNAi Kit (catalog no. P1700, Promega) (Li et al. 2018; Zhu et al. 2020). The siRNAs were obtained by digesting dsRNAs with ShortCut RNase III (catalog no. M0245S, New England Biolabs) to ~21 nt fragments (siRNAs). Briefly, 40  $\mu$ g

of dsRNA was digested with ShortCut RNase III in a 100  $\mu$ l reaction at 37 °C for 30 min. Ten microliters of 10 $\times$  EDTA (0.5 M) was added to stop the reaction, and the small RNAs were precipitated with ethanol and dissolved in ddH<sub>2</sub>O.

A female adult of *P. americana* was injected with 2  $\mu$ l of 2  $\mu$ g/ $\mu$ l *PRP* and *GRP* dsRNA or *laccase 2* siRNA on days 4, 6, and 8 PAE. For *Vg* RNAi, injections twice on days 6 and 8 PAE were performed to avoid RNAi knockdown of *Vgs* in the fat body.

### High-Temperature Stress

Changes in ootheca weight were used to test water retention capability under high-temperature stress. Fresh oothecae ( $n = 30$ ) were placed in sterile Petri dishes (9 cm diameter) at 30, 37, and 44 °C. The weights of oothecae were recorded at 24-h intervals for 7 days, and the distorted oothecae were recorded for at least one month.

## Measurements

The control and treated oothecae were photographed with a Nikon DS-Ri2 camera and analyzed with a Nikon SMZ25 microscope. After cryostat sectioning, the thickness of oothecae was measured by using Adobe Photoshop CS6. The weight of oothecae was also measured. For the color assay, the images were read and modified by Adobe Camera Raw and corrected by the 24-Patch Color Checker chart in Adobe DNG Profile Editor. Photoshop was used to estimate the values of RGB channels (RGB for red, green, and blue, respectively, as below), and the difference in color was further statistically analyzed (Zhang et al. 2003). Daily assays of the water retention ability of oothecae were based on weight changes at a fixed temperature and humidity.

## Biochemical and Molecular Methods

### Quantitative Real-Time PCR

Total RNA was isolated from CGs and fat body of *P. americana*. qPCR was performed in triplicate using SYBR Premix Ex Taq™ II (Takara, Dalian, China). The expression of beta-actin ( $\beta$ -actin) was quantified as a reference for normalization. The relative expression levels of target genes were calculated by using the  $\Delta\Delta$ Ct method following the manufacturer's instructions (Li et al. 2019; Zhu et al. 2020). The primers are listed in [supplementary table S2, Supplementary Material online](#).

### SDS-PAGE

Fresh oothecae were collected as the insects oviposited and immediately placed in liquid nitrogen. Freshly extruded oothecae, regarded as day 1 oothecae, could be easily dissolved in RIPA buffer containing 1 mM phenylmethanesulfonyl fluoride before they hardened. Solubilized proteins from fresh oothecae and mature CGs were analyzed by 12% SDS-PAGE (Zhu et al. 2020).

### Antibody Generation and Western Blotting

The rabbit polyclonal antibody against Vg1 or Vg2 was generated by immunization of rabbits with purified histidine-

tagged Vg1 or Vg2 fusion protein (ABclonal Biotech). For Western blotting, all primary antibodies were diluted to 1/1,000, and secondary antibodies (goat anti-rabbit IgG-HRP) were diluted to 1/2,000. The density of Vg bands was quantified with the image analysis software ImageJ (Tian et al. 2013; Zhu et al. 2020).

### Proteomics

Five slices of bands from SDS–PAGE separating the newly laid oothecae of *P. americana* (fig. 1C) were subjected to in-gel protein digestion. CGs and oothecae were harvested from egg-laying female insects, and total proteins were extracted with urea lysis buffer (8 M urea with 1% SDS) containing 1 mM PMSF. LC-MS/MS analysis was carried out on a Dionex Ultimate 3000 RSLCnano (Thermo Scientific, MA) coupled with a Q-Exactive mass spectrometer (Thermo Fisher Scientific, MA). Protein identification was performed with MaxQuant by searching the UniProt database and three species' databases (*H. patellifera*, <https://www.ncbi.nlm.nih.gov/sra/PRJNA707485>; *L. migratoria*, <http://159.226.67.243/download.htm>; *P. americana*, <https://www.ncbi.nlm.nih.gov/Traces/wgs/PGRX01?display=contigs>). Proteins were searched against the GO, KEGG, and COG/KOG databases to be categorized by different functions and pathways. Significant GO functions and pathways were determined within differentially expressed proteins at a  $P$  value  $\leq 0.05$ . The alignments and structure prediction of proteins were performed with the software Jalview and Phyre2 online (<http://www.sbg.bio.ic.ac.uk/~phyre2/html/>), respectively.

### Metabolomics

#### Metabolite Extraction

Metabolite extraction was performed using a methanol solvent mixture and an internal target. Briefly, the sample was homogenized in a ball mill for 4 min at 45 Hz and then ultrasonicated on ice. After incubating for 1 h at  $-20^{\circ}\text{C}$  to precipitate proteins and centrifuging at 12,000 rpm for 15 min at  $4^{\circ}\text{C}$ , the supernatant was dried in a vacuum concentrator without heating, and extraction buffer was added for reconstitution. The mixture was vortexed for 30 s, sonicated for 10 min, and centrifuged for 15 min at 12,000 rpm and  $4^{\circ}\text{C}$ . The supernatant was transferred into a fresh 2 mL LC/MS glass vial for UHPLC-QTOF-MS analysis. Equal amounts of each sample were pooled as QC samples (Bar et al. 2020).

#### LC-MS/MS Analysis

LC-MS/MS analyses were performed using a UPLC system (1290, Agilent Technologies), a UPLC BEH Amide column, and a TripleTOF 6600 instrument (Q-TOF, AB Sciex). The mobile phase consisted of  $\text{NH}_4\text{OAc}$  and  $\text{NH}_4\text{OH}$  in water and an acetonitrile elution gradient. A  $3\text{-}\mu\text{l}$  volume was injected. During each LC/MS experiment, the triple TOF mass spectrometer acquired MS/MS spectra on an information-dependent basis (IDA).

Metabolites were identified by searching the KEGG database and analyzed by Metabolite Set Enrichment Analysis (MSEA; <https://rdrr.io/github/afukushima/MSEAp/>) and

quantitative enrichment analysis based on the SMPDB database (The Small Molecule Pathway Database; <https://smpdb.ca>). The metabolomics data have been deposited to the MetaboLights database (<https://www.ebi.ac.uk/metabolights/editor/study/MTBLS3524>).

### Bioinformatics Analyses

#### Venn Diagram Construction

Based on the known metabolites or proteins, common or specific data sets of proteins or metabolites between or among the tissues were obtained and presented as a Venn diagram for visualization.

#### Principal Component Analysis

To visualize the differences between groups, the unsupervised dimensionality reduction method of principal component analysis was applied to all samples using R package models (<http://www.r-project.org/>).

#### Heatmap Construction

A heatmap was created in which expression level is colored according to the known shared metabolites or proteins among the tissues within or among the species.

#### Differential Metabolite Analysis

Differential metabolites were searched based on the variable importance in projection (VIP) score of the (O) PLS model. A  $t$ -test was applied for univariate analysis to screen differential metabolites. Metabolites with a  $P$  value of  $t$ -test  $< 0.05$  and  $\text{VIP} \geq 1$  were considered differential metabolites between two groups.

#### KEGG Pathway Analysis

Metabolites were annotated against the KEGG database. Significantly enriched metabolomic pathways of differential metabolites were compared with the whole background. Pathways were regarded as significantly enriched pathways of differential metabolites when the corrected  $P$  value was below the threshold of  $\text{FDR} \leq 0.05$ .

#### Correlation Analysis of Proteomics and Metabolomics Data

Proteins and metabolites were used to integrate the significantly enriched KEGG pathways related to OSP sclerotization and melanization. Differential metabolites and differentially expressed proteins are highlighted with colors. The biological pathways and functions of interest associated with the differentially abundant molecules were further studied based on the KEGG pathway mapper.

#### Statistical Analysis

Statistical analyses were performed with Student's  $t$ -test or one-way ANOVA or two-way ANOVA. Values are shown as the mean  $\pm$  standard error ( $M \pm \text{SE}$ ), and differences were considered significant at  $P < 0.05$ ,  $P < 0.01$ ,  $P < 0.001$ .

## Supplementary Material

Supplementary data are available at *Molecular Biology and Evolution* online.

## Acknowledgments

We are grateful for Dr Xiaoqiang Yu and Dr Erjun Ling for their comments on studies of sclerotization and melanization. This work was supported by Laboratory of Lingnan Modern Agriculture Project (NT2021003) and National Science Foundation of China (31930014 and 316201039170) to S.L.; National Science Foundation of Guangdong Province of China (2021A515011363) to E.D.; National Science Foundation of China (31970438) to Y.X.L.; National Science Foundation of China (31900355) to N.L.; National Science Foundation of China (U1804232) to S.Z.; and Department of Science and Technology in Guangdong Province (2019B090905003 and 2019A0102006) and Shenzhen Science and Technology Program (20180411143628272) to S.L.

## Author Contributions

Conceptualization: S.L. Methodology: E.D., Y.X.L., S.W., C.Z., W.M., Y.C., D.Y., Z.L. Investigation: E.D., Y.X.L., S.W., C.Z., Z.L. Visualization: E.D., C.D., Y.X.L., T.Z. Supervision: S.L., N.L., S.Z., S.R. Writing—original draft: E.D., S.L. Writing—review and editing: S.L., S.R., N.L., S.Z., E.D., Y.X.L., J.Z., G.W., C.R., T.Z.

## Data Availability

The raw mass spectrometry proteomics data have been deposited to the ProteomeXchange Consortium (<http://proteomecentral.proteomexchange.org>) via the iProX partner repository with the data set identifier IPX0003543000. The raw metabolomics data have been deposited to the MetaboLights database (<https://www.ebi.ac.uk/metabolights/editor/study/MTBLS3524>).

## References

Andersen SO. 2010. Insect cuticular sclerotization: a review. *Insect Biochem Mol Biol.* 40(3):166–178.

Arndt EM, Moore W, Lee WK, Ortiz C. 2015. Mechanistic origins of bombardier beetle (Brachinini) explosion-induced defensive spray pulsation. *Science* 348(6234):563–567.

Babin PJ, Bogerd J, Kooiman FP, Van Marrewijk WJ, Van der Horst DJ. 1999. Apolipophorin II/I, apolipoprotein B, vitellogenin, and microsomal triglyceride transfer protein genes are derived from a common ancestor. *J Mol Evol.* 49(1):150–160.

Bar N, Korem T, Weissbrod O, Zeevi D, Rothschild D, Leviatan S, Kosower N, Lotan-Pompan M, Weinberger A, Le Roy Cl, et al. 2020. A reference map of potential determinants for the human serum metabolome. *Nature* 588(7836):135–140.

Bell WJ, Adiyodi KG. 1981. *The American cockroach*. London: Chapman and Hall.

Benton MJ. 2016. The Triassic. *Curr Biol.* 26:1214–1218.

Carigliano B, Lara MB, Zavattieri AM. 2020. Earliest record of fossil insect oothecae confirms the presence of crown-dictyopteran taxa in the Late Triassic. *Syst Entomol.* 45:935–947.

Cassab GI. 1998. Plant cell wall proteins. *Annu Rev Plant Physiol Plant Mol Biol.* 49:281–309.

Chen N, Pei XJ, Li S, Fan YL, Liu TX. 2020. Involvement of integument-rich CYP4G19 in hydrocarbon biosynthesis and cuticular penetration resistance in *Blattella germanica* (L.). *Pest Manag Sci.* 76(1):215–226.

Church SH, Donoughe S, de Medeiros BAS, Extavour CG. 2019. Insect egg size and shape evolve with ecology but not developmental rate. *Nature* 571(7763):58–62.

Coelho MT, Diniz-Filho JA, Rangel TF. 2019. A parsimonious view of the parsimony principle in ecology and evolution. *Ecography* 42(5):968–976.

Courrent A, Quenedey A, Nalepa CA, Robert A, Lenz M, Bordereau C. 2008. The fine structure of colleterial glands in two cockroaches and three termites, including a detailed study of *Cryptocercus punctulatus* (Blattaria, Cryptocercidae) and *Mastotermes darwiniensis* (Isoptera, Mastotermitidae). *Arthropod Struct Dev.* 37(1):55–66.

Crisi JV. 1982. Parsimony in evolutionary theory: law or methodological prescription? *J Theor Biol.* 97(1):35–41.

Dittmer NT, Kanost MR. 2010. Insect multicopper oxidases: diversity, properties, and physiological roles. *Insect Biochem Mol Biol.* 40(3):179–188.

Flowers RW, Chaboo CS. 2015. Natural history of the tortoise beetle, *Discomorpha* (Discomorpha) *biplagiata* (Guérin) (Chrysomelidae: Cassidinae: Omocerini). *Imago Mundi.* 439:1–10.

Gillott C. 2005. *Entomology*. New York: Plenum Press.

Goldberg J, Bresseel J, Constant J, Kneubuhler B, Leubner F, Michalik P, Bradler S. 2015. Extreme convergence in egg-laying strategy across insect orders. *Sci Rep.* 5:7825.

Grimaldi D, Engel MS. 2005. *Evolution of the insects*. New York: Cambridge University Press.

Hopkins TL, Starkey SR, Xu R, Merritt ME, Schaefer J, Kramer KJ. 1999. Catechols involved in sclerotization of cuticle and egg pods of the grasshopper, *Melanoplus sanguinipes*, and their interactions with cuticular proteins. *Arch Insect Biochem Physiol.* 40(3):119–128.

Hörnig MK, Haug C, Schneider JW, Haug JT. 2018. Evolution of reproductive strategies in dictyopteran insects—clues from ovipositor morphology of extinct roachoids. *Acta Palaeontol Pol.* 63:1–24.

Howard RW, Blomquist GJ. 2005. Ecological, behavioral, and biochemical aspects of insect hydrocarbons. *Annu Rev Entomol.* 50:371–393.

Huang J, Miller JR, Chen SC, Vulule JM, Walker ED. 2006. *Anopheles gambiae* (Diptera: Culicidae) oviposition in response to agarose media and cultured bacterial volatiles. *J Med Entomol.* 43(3):498–504.

Hunt L, Amsbury S, Baillie A, Movahedi M, Mitchell A, Afsharinafar M, Swarup K, Denyer T, Hobbs JK, Swarup R, et al. 2017. Formation of the stomatal outer cuticular ledge requires a guard cell wall proline-rich protein. *Plant Physiol.* 174(2):689–699.

Jayadev R, Sherwood DR. 2017. Basement membranes. *Curr Biol.* 27:199–217.

John ME, Keller G. 1995. Characterization of mRNA for a proline-rich protein of cotton fiber. *Plant Physiol.* 108(2):669–676.

Küpper SC, Klass KD, Uhl G, Eberhard MJB. 2019. Comparative morphology of the internal female genitalia in two species of Mantophasmatodea. *Zoomorphology* 138(1):73–83.

Leipart V, Montserrat-Canals M, Cunha ES, Luecke H, Herrero-Galán E, Halskau Ø, Amdam GV. 2022. Structure prediction of honey bee vitellogenin: a multi-domain protein important for insect immunity. *FEBS Open Bio.* 12 (1):51–70.

Li J, Christensen BM. 1993. Involvement of L-tyrosine and phenol oxidase in the tanning of *Aedes aegypti* eggs. *Insect Biochem Mol Biol.* 23(6):739–748.

Li N, Zeng M, Xiao H, Lin S, Yang S, Huang H, Zhu S, Zhao Z, Ren C, Li S. 2019. Alteration of insulin and nutrition signal gene expression or depletion of Met reduce both lifespan and reproduction in the German cockroach. *J Insect Physiol.* 118:103934.

Li S, Zhu S, Jia Q, Yuan D, Ren C, Li K, Liu S, Cui Y, Zhao H, Cao Y, et al. 2018. The genomic and functional landscapes of developmental plasticity in the American cockroach. *Nat Commun.* 9(1):1008.

Machida R, Tojo K, Tsutsumi T, Uchifune T, Pretorius L. 2004. Embryonic development of heel-walkers: reference to some prerevolutionary stages (Insecta: Mantophasmatodea). *Proc Arthropod Embryol Soc Jpn.* 39:31–39.

Malek R, Kaser JM, Broadley HJ, Gould J, Ciolli M, Anfora G, Hoelmer KA. 2019. Footprints and ootheca of *Lycorma delicatula* influence host-

- searching and-acceptance of the egg-parasitoid *Anastatus orientalis*. *Environ Entomol.* 48(6):1270–1276.
- Marinotti O, Ngo T, Kojin BB, Chou SP, Nguyen B, Juhn J, Carballar-Lejarazu R, Marinotti PN, Jiang X, Walter MF, et al. 2014. Integrated proteomic and transcriptomic analysis of the *Aedes aegypti* eggshell. *BMC Dev Biol.* 14:15.
- Matsuoka Y, Monteiro A. 2018. Melanin pathway genes regulate color and morphology of butterfly wing scales. *Cell Rep.* 24(1):56–65.
- Mettlen M, Chen PH, Srinivasan S, Danuser G, Schmid SL. 2018. Regulation of clathrin-mediated endocytosis. *Annu Rev Biochem.* 87:871–896.
- Misof B, Liu S, Meusemann K, Peters RS, Donath A, Mayer C, Frandsen PB, Ware J, Flouri T, Beutel RG, et al. 2014. Phylogenomics resolves the timing and pattern of insect evolution. *Science* 346(6210):763–767.
- Miyazaki S, Shimoji H, Suzuki R, Chinushi I, Takayanagi H, Yaguchi H, Miura T, Maekawa K, Yaguchi H. 2021. Expressions of conventional vitellogenin and vitellogenin-like A in worker brains are associated with a nursing task in a ponerine ant. *Insect Mol Biol.* 30(1):113–121.
- Mousavi A, Hotta Y. 2005. Glycine-rich proteins – a class of novel proteins. *Appl Biochem Biotechnol.* 120(3):169–174.
- Mullins DE, Mullins KJ, Tignor KR. 2002. The structural basis for water exchange between the female cockroach (*Blattella germanica*) and her ootheca. *J Exp Biol.* 205(Pt 19):2987–2996.
- Needham JG, Heywood HB. 1929. Handbook of dragonflies of North America. Baltimore (MD): C.C. Thomas.
- Needham JG, Westfall JM. 1955. A manual of dragonflies of North American. Berkeley (CA): Berkeley University of California Press.
- Nicholson DB, Ross AJ, Mayhew PJ. 2014. Fossil evidence for key innovations in the evolution of insect diversity. *Proc Biol Sci.* 281:1–7.
- Noh MY, Muthukrishnan S, Kramer KJ, Arakane Y. 2016. Cuticle formation and pigmentation in beetles. *Curr Opin Insect Sci.* 17:1–9.
- Pinski A, Betekhtin A, Sala K, Godel-Jedrychowska K, Kurczynska E, Hasterok R. 2019. Hydroxyproline-rich glycoproteins as markers of temperature stress in the leaves of *Brachypodium distachyon*. *Int J Mol Sci.* 20:1–21.
- Raikhel AS. 2005. Vitellogenesis of disease vectors, from physiology to genes. In: Marquardt WC, editor. Biology of disease vectors. London, United Kingdom: Elsevier Academic Press. p. 329–346.
- Ringli C, Keller B, Ryser U. 2001. Glycine-rich proteins as structural components of plant cell walls. *Cell Mol Life Sci.* 58:1430–1441.
- Roth S, Molina J, Predel R. 2014. Biodiversity, ecology, and behavior of the recently discovered insect order Mantophasmatodea. *Front Zool.* 11(1):1–20.
- Sugumaran M, Berek H. 2016. Critical analysis of the melanogenic pathway in insects and higher animals. *I J Mol Sci.* 17(10):1753–1777.
- Tanner LH, Lucas SG, Chapman MG. 2004. Assessing the record and causes of Late Triassic extinctions. *Earth Sci Rev.* 65(1–2):103–139.
- Terrapon N, Li C, Robertson HM, Ji L, Meng XH, Booth W, Chen ZS, Childers CP, Glastad KM, Gokhale K, et al. 2014. Molecular traces of alternative social organization in a termite genome. *Nat Commun.* 5:3636.
- Tian L, Ma L, Guo E, Deng X, Ma S, Xia Q, Cao Y, Li S. 2013. 20-Hydroxyecdysone upregulates Atg genes to induce autophagy in the *Bombyx* fat body. *Autophagy* 9(8):1172–1187.
- Tojo K, Machida R, Klass KD, Picker MD. 2004. Biology of South African heel-walkers, with special reference to reproductive biology (Insecta: Mantophasmatodea). *Proc Arthropod Embryol Soc Jpn.* 39:15–21.
- Tseng IC, Hong CY, Yu SM, Ho THD. 2013. Abscisic acid- and stress-induced highly proline-rich glycoproteins regulate root growth in rice. *Plant Physiol.* 163(1):118–134.
- Walker AA, Weisman S, Kameda T, Sutherland TD. 2012. Natural templates for coiled-coil biomaterials from praying mantis egg cases. *Biomacromolecules* 13(12):4264–4272.
- Whitehead DL. 2011. Haemocytes play a commensal role in the synthesis of the dihydroxybenzoate required as a precursor for sclerotization of the egg case (ootheca) in the cockroach *Periplaneta americana* (L). *Bull Entomol Res.* 101(3):251–258.
- Willis JH. 2010. Structural cuticular proteins from arthropods: annotation, nomenclature, and sequence characteristics in the genomics era. *Insect Biochem Mol Biol.* 40(3):189–204.
- Wipfler B, Letsch H, Frandsen PB, Kapli P, Mayer C, Bartel D, Buckley TR, Donath A, Edgerly-Rooks JS, Fujita M, et al. 2019. Evolutionary history of Polyneoptera and its implications for our understanding of early winged insects. *Proc Natl Acad Sci U S A.* 116(8):3024–3029.
- Yarawsky AE, English LR, Whitten ST, Herr AB. 2017. The proline/glycine-rich region of the biofilm adhesion protein Aap forms an extended stalk that resists compaction. *J Mol Biol.* 429(2):261–279.
- Young HP, Larabee JK, Gibbs AG, Schal C. 2000. Relationship between tissue-specific hydrocarbon profiles and lipid melting temperatures in the cockroach *Blattella germanica*. *J Chem Ecol.* 26(5):1245–1263.
- Zhang J, Goyer C, Pelletier Y. 2008. Environmental stresses induce the expression of putative glycine-rich insect cuticular protein genes in adult *Leptinotarsa decemlineata* (Say). *Insect Mol Biol.* 17(3):209–216.
- Zhang M, De Baerdemaeker J, Schrevels E. 2003. Effects of different varieties and shelf storage conditions of chicory on deteriorative color changes using digital image processing and analysis. *Food Res Int.* 36(7):669–676.
- Zhu S, Liu F, Zeng H, Li N, Ren C, Su Y, Zhou S, Wang G, Palli SR, Wang J, et al. 2020. Insulin/IGF signaling and TORC1 promote vitellogenesis via inducing juvenile hormone biosynthesis in the American cockroach. *Development* 147(20):1–13.